energies

Article

Fault Detection and Power Loss Assessment for Rooftop Photovoltaics Installed in a University Campus, by Use of UAV-Based Infrared Thermography

Kyoik Choi and Jangwon Suh *

Department of Energy and Mineral Resources Engineering, Kangwon National University, Samcheok 25913, Republic of Korea; rydlr3020@naver.com
* Correspondence: jangwonsuh@kangwon.ac.kr or jangwonsuh@hanmail.net; Tel.: +82-33-570-6313

Abstract: In contrast to commercial photovoltaic (PV) power plants, PV systems at universities are not actively monitored for PV module failures, which can result in a loss of power generation. In this study, we used thermal imaging with drones to detect rooftop PV module failures at a university campus before comparing reductions in power generation according to the percentage of module failures in each building. Toward this aim, we adjusted the four factors affecting the power generation of the four buildings to have the same values (capacities, degradations due to aging, and the tilts and orientation angles of the PV systems) and calibrated the actual monthly power generation accordingly. Consequently, we detected three types of faults, namely open short-circuits, hot spots, and potential-induced degradation. Furthermore, we found that the higher the percentage of defective modules, the lower the power generation. In particular, the annual power generation of the building with the highest percentage of defective modules (12%) was reduced by approximately 25,042 kWh (32%) compared to the building with the lowest percentage of defective modules (4%). The results of this study can contribute to improving awareness of the importance of detecting and maintaining defective PV modules on university campuses and provide a useful basis for securing the sustainability of green campuses.

Keywords: module fault; thermal infrared thermography; rooftop photovoltaic; green campus; sustainability

check for updates

Citation: Choi, K.; Suh, J. Fault Detection and Power Loss Assessment for Rooftop Photovoltaics Installed in a University Campus, by Use of UAV-Based Infrared Thermography. *Energies* **2023**, *16*, 4513. https://doi.org/10.3390/en16114513

Academic Editor: Luigi Vesce

Received: 18 April 2023
Revised: 22 May 2023
Accepted: 2 June 2023
Published: 4 June 2023

1. Introduction

Several types of defects have been found in photovoltaic (PV) modules which reduce the module power output, preventing modules from reversing to normal behavior and causing safety issues [1]. The most common panel failures are delamination, loss of backsheet adhesion, bad junction boxes, broken frames, ethyl vinyl acetate discoloration, cell cracks, snail marks, burn marks, potential-induced degradation (PID), breaks in cell- and string-interconnect ribbons, defective bypass diodes, micro-arcing in connectors, shunt hot spots, broken front glass, and degraded back contact electrodes [2]. Product failures are generally divided into three categories: infant failure, midlife failure, and wear out. Initial failures generally occur at the beginning of a panel's operational life, with the most important failures in the field being junction box failures, glass breakage, cell interconnect defects, frame looseness, and delamination. Additionally, mid-panel failures show that the incidence of defective interconnects within modules is significantly higher, whilst panel failures due to glass breakage are also high. The relative failure rates of the junction boxes and cables, cell burn marks, and packaging materials were all relatively high. Aging failures typically occur at the end of a panel's operational life and determine its maximum operational life. The main failures of the modules were delamination, separation of cell pieces owing to cell cracking, and discoloration of the laminate [3,4].

To ensure the sustainability of PV power generation facilities, it is necessary to monitor and minimize the loss of power generation due to defective modules. In the case of commercial PV power plants, continuous monitoring, inspection, and maintenance are actively carried out since they are operated for maximizing power generation. Conversely, detection and maintenance of module failures are not sufficient in schools and public institutions that do not have a commercial purpose for PV power generation systems since these require significant time and costs [5]. Rooftop PV systems are installed under the mandatory renewable energy portfolio standard in the Republic of Korea, which requires that public institutions and local governments obtain a certain percentage of their energy from new and renewable energy sources (32% or more by 2022) in buildings with an area of 1000 m^2 or more that are newly built, expanded, or renovated [6]. Moreover, there are many examples of green campuses worldwide that have PV systems (e.g., South Korea [5], Indonesia [7], Japan [8], India [9], Nepal [10], China [11], Vietnam [12], Pakistan [13], USA [14], Mexico [15], Brazil [16], Italy [17], and Nigeria [18]). Therefore, it is necessary to detect defects in PV modules through periodic inspection and monitoring and to prevent power generation degradation through the maintenance of PV systems installed on university campuses.

Researchers worldwide have conducted studies on the detection of defective PV modules. The International Energy Agency's Photovoltaic Power Systems Program summarizes the types and details of PV module failures/faults described in infrared thermography. This enables the determination of the type of defect or risk from a thermal image of a PV module. Unmanned aerial vehicles (UAVs) have often been used to monitor PV plants at a local scale (<1 km^2) [19–27]. Several studies have been proposed aiming to automatically derive the line or region of PV modules using thermal imaging drones [19–21] based on computer vision technology, evaluate high-resolution UAV imagery for overhauling large-scale PV power plants [22–24], or analyze the suitability of irradiation according to the tilt angle of PV modules in drone-based PV power plant monitoring [25]. Many studies have previously reported the use of drones equipped with only thermal imaging cameras [26–31] or both thermal and optical imaging cameras [32–35] to inspect defects of PV modules. More recently, research has been reported that adopts artificial intelligence (AI) technology (e.g., convolutional neural networks, naive Bayes classifiers) in detecting or monitoring PV module failures. The combined use of drone-based thermal infrared imaging and AI technology (i.e., machine learning and deep learning) has the advantage of not only reducing the time and cost of monitoring large-scale PV power plants, but also detecting defects automatically with high accuracy [36–41]. However, the majority of these studies were limited to detecting inspections or defects in PV power generation systems, whilst there remains a lack of studies analyzing the actual power generation degradation resulting from PV module defects. Considering that the detection of PV module failures is aimed at reducing power generation losses through maintenance, it is necessary to conduct a study that can detect PV module failures in addition to analyzing the amount of power generation degradation these module failures have caused.

The objective of this study is to analyze reductions in power generation for campus rooftop photovoltaics through module faults detected using UAV-based thermal infrared images. Toward this aim, we quantitatively analyze the amount of power generation loss caused by passive maintenance after detecting defects in the rooftop PV systems of each building on a university campus and evaluate the types and rates of module defects, using drone-based thermal images to determine the causes. This study differs from existing research in that it can contribute to improving awareness of the need for the active maintenance of energy infrastructure to create a sustainable green campuses under challenging circumstances for university campuses which lack necessary funding.

2. Study Area

The Samcheok Campus of Kangwon National University was selected as the research area for this study to analyze the defect detection and power generation degradation of

PV modules by using thermal imaging drones. Kangwon National University Samcheok Campus is located in Samcheok City, Gangwon-do, South Korea, at 37°27′07.9″ N latitude and 129°09′42.8″ E longitude.

Originally, six of the 26 buildings on campus were equipped with rooftop PV modules (silicon-based). However, considering the quantity and quality of the power generation data for each building monitored here, only four buildings (named building E5, building E4, building J, and building G) were selected for analysis, as shown in Figure 1. The installation time (for calculating aging), design capacity, performance degradation, tilt angle, and azimuthal angle of each facility all differed significantly (Table 1). The PV facilities in the study area have been in operation for a minimum of one year and a maximum of 15 years, with design capacities ranging from 50 to 100 kW_P. In case of module performance degradation, they start out with 96–98% performance in the first year of operation and performance decreases by 0.3–0.8%p per year as they age. The module performance change through aging is an internal characteristic that is present when the module is produced by its manufacturer. The performance degradation formula for the modules installed in each building based on the operating period is shown in Table 1. The four engineering buildings were composed of four strings with two types of tilt angles. The remaining three buildings, except for building G, had an azimuth angle of 142° because the PV modules were installed parallel to the building's rooftop boundary instead of facing south. In the case of the rooftop PV modules of building G, the installation tilt angle was 14° instead of 25° (optimal). This is because the effect of the shadow from the front array installed on the rooftop on the rear array was minimized and the design of the structure was problematic. Details on the specifications of the PV modules for each building are summarized in Table 2.

Table 1. Information on the rooftop PV systems at Kangwon National University.

Building Name	Rooftop PV System					
	Operation	Type	Capacity (kW_p)	Degradation (%) *	Tilt (°)	Azimuth (°)
E5	December 2018~present	Fixed	100.00 (=400 W × 250 EA)	$98.5 - 0.5 \times$ age (yr)	23	142
E4	September 2021~present	Fixed	70.84 (=460 W × 154 EA)	$96 - 0.67 \times$ age (yr)	25, 15	142
G	January 2020~present	Fixed	67.60 (=400 W × 169 EA)	$98 - 0.5 \times$ age (yr)	14	180
J	Jan 2008~present	Fixed	50.00 (=173 W × 290 EA)	$97 - 0.8 \times$ age (yr)	25	142

* This does not refer to photoelectric efficiency, but rather to performance over age.

Table 2. Specifications of the PV modules installed at Kangwon National University.

Module	Building Name			
Specification	E5	E4	G	J
Model	LG400N2W-A5	Q.PEAK DUO XL-G9.3 460	LG400N2W-A5	SE-S173
Rated maximum power (P_{max}) [W]	400	460	400	173
Open circuit voltage (V_{oc}) [V]	49.3	53.66	49.3	43.9
Maximum power voltage (V_{mp}) [V]	40.6	45.44	40.6	36.6
Short circuit current (I_{sc}) [A]	10.47	10.63	10.47	5.13
Maximum power current (I_{mp}) [A]	9.86	10.12	9.86	4.73
Efficiency [%]	19.3	20.6	19.3	13.9

Since the four buildings were spaced apart and had similar rooftop elevations, the PV modules were not affected by shadows from the surrounding terrain or buildings. Furthermore, there are structures such as roof entrances in addition to PV modules on the rooftops of buildings E5, J, and G. However, in the case of buildings E5 and J, the shadow effect of the module was insignificant because the structure is located to the north of the module. In the case of building G, there is a structure on the right, but there is greater distance from the array on the left (which can affect shadows), so the shadow effect was minimized. Therefore, it is considered that the shadow effect on the rooftop PV in this study area is very low. Currently, the rooftop PV facilities are operated and maintained by the Campus Facilities Support Division.

Figure 1. Aerial photographs of the rooftop PV at Kangwon National University, Republic of Korea (image from: http://www.google.com/maps (accessed on 1 June 2023)).

3. Methods

In this study, we analyzed the defect detection and power generation degradation of PV modules using a thermal imaging drone, following the procedure shown in Figure 2. Firstly, thermal images of the PV modules were acquired using a drone thermal imaging camera, whilst suspected defective modules were detected by considering the relative temperature difference characteristics and patterns of the modules. In addition, we adjusted the design capacity, the amount of degradation of the modules' power generation efficiency over the operating period, and the tilt and azimuth characteristics of the PV power generation facilities in the four buildings to be the same whilst also calibrating the monthly power generation accordingly. We then analyzed the impacts of defective PV modules on the degradation of power generation by comparing the percentage of defective core modules between buildings and the power generation correction values.

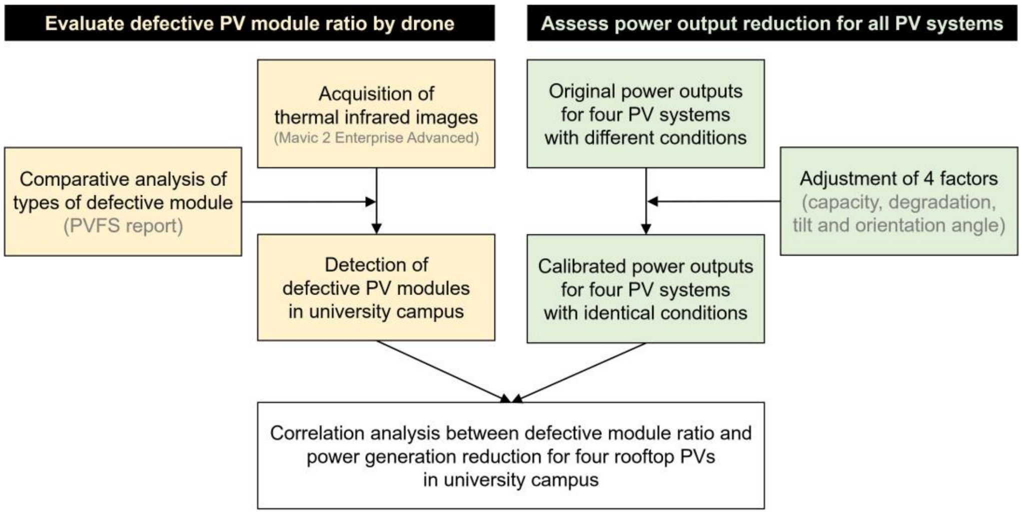

Figure 2. Flowchart for the analysis of defective modules and power generation reduction.

3.1. Detection of PV Module Failures with a Thermal Imaging Drone

In this study, the MAVIC 2 Enterprise Advanced (hereafter MAVIC 2) drone developed by Da Jiang Innovation (DJI) was used to acquire the thermal characteristics of rooftop PV modules. The MAVIC 2 drone has advantages such as an integrated high-resolution thermal imaging sensor used to quickly recognize objects in the field. It is also equipped with a visible light camera and a thermal imaging camera on a stabilized three-axis gimbal to provide visible and infrared images simultaneously (Table 3).

Standards from the International Electrotechnical Commission (IEC) were consulted for the acquisition and analysis of the thermal images of the photovoltaic modules [42]. IEC TS 62446-3:2017 (E) defines the requirements for the outdoor thermal imaging inspection of photovoltaic power plants in operation. Thermal images with a spatial resolution of 3 cm/pix were acquired in accordance with the IEC standards to obtain sufficient samples for the measured temperatures for all PV cells. Weather conditions such as temperature, humidity, wind, precipitation, and sunlight were all considered when selecting a drone flight date; flights were conducted at approximately 10 a.m. and 3 p.m., avoiding times such as 2 h after sunrise (low temperatures reduce accuracy), midday (strong light causes reflections), and 2 h before sunset (shadow issues).

For stable and standardized data collection, we used an autoflight function supported by the Pix4D capture application to fly and capture the drone. The drone-based images were taken from a height of 30 m above the altitude of each building's rooftop PV modules in order to clearly distinguish the temperature differences between cells within a module and temperature distributions within cells. The surface emissivity was set to a typical value of 0.9. In addition, the temperature measurement range of each building's rooftop PV modules was set automatically, as each type of PV module failure has a different temperature distribution and pattern.

To detect PV module failures, characterization of the relative temperature distribution or pattern within the module as seen in the thermal image was analyzed. For this, various types of PV module failures presented in the photovoltaic failure fact sheet (PVFS) [1] of the Photovoltaic Power Systems Program of the International Energy Agency (IEA PVPS) Task 13 were compared and analyzed using thermal images taken in the study area.

Table 3. Specifications of the DJI Mavic 2 Enterprise Advanced [43].

Type	Features	Performance
Aircraft	Dimensions (L × W × H) Takeoff weight (Without accessories)	Folded: 214 × 91 × 84 mm^3 Unfolded: 322 × 242 × 84 mm^3
	Max. speed	72 kph (S-mode, without wind)
	Max. flight time	31 min (measured while flying at 25 kph in windless conditions)
M2EA Thermal Camera	Sensor resolution Digital zoom Accuracy of thermal temperature	640 × 512 @30Hz 16× Measurement: ±2 °C or ±2%, whichever is greater.

3.2. Comparative Analysis of Reduction in Power Generation by Building

At the Kangwon National University Samcheok Campus, the rooftop PV system monitors power generation from the time of operation. As mentioned above, building J has been operating for approximately eleven years (January 2012 to December 2022), while building E4 has approximately one year of data (2022). Therefore, to compare the power generation degradation in each building due to the failure rate of PV modules, this study used the monthly power generation from 2022, for which data are available for all buildings, as a reference value.

To compare the power generation degradation owing to PV module failure, the weather conditions and system design factors (characteristic values) must be the same for all other conditions. In the case of the study area, since the area was within 0.3 km^2, the weather conditions can be assumed to be the same, while characteristic values such as the capacity of the PV system by building, the module power generation efficiency according to the operating period, and the tilt and azimuth angles were different (Table 1).

The PV installation capacity was proportional to the power generation. For example, all else being equal, the 50 kW$_p$ facility will generate half as much electricity as the 100 kW$_p$ facility. Considering that silicon-based PV modules generally lose efficiency at a rate of approximately 0.3–0.8% per year, it is necessary to adjust the power-generation efficiency of PV modules in buildings with different installation years to be the same. We obtained the annual degradation rate data for each module by contacting the module manufacturer in the Republic of Korea. For example, modules installed in building E5 had a first-year power generation performance of 98.5%, and after four years of operation (as shown in Table 1) their performance would be 96.5%. The tilt and azimuth angles can both affect power generation, depending on the angle of incidence of the sun.

Therefore, in this study, the other conditions (influencing factors) were adjusted equally, as shown in Table 4, to analyze only the power-generation degradation caused by the failure of the PV modules. For the entire building, the installed capacity of the modules was set to 50 kW$_P$, the degradation of the power generation efficiency of the module owing to the time of installation was set to 0%, the tilt angle was set to 25°, and the azimuth angle was set to 142°. Thus, the monthly power generation of each building could compensate for the changes in the values of the four influencing factor characteristics.

Table 4. Property modification of rooftop PV systems for analysis of the reduction in power output.

Building Name	Capacity (kW$_P$)		Degradation by Year (%) *		Tilt (°)		Azimuth (°)	
	Original	Revised	Original	Revised	Original	Revised	Original	Revised
E5	100.00	50	96.50	100	23	25	142	142
E4	70.84		95.30		25, 15		142	
G	67.60		96.50		14		180	
J	50.00		88.20		25		142	

* This does not refer to photoelectric efficiency, but rather to performance over age.

4. Results & Interpretations

4.1. Detecting PV Panel Failures Using Thermal Imaging Drones

Figure 3 shows the thermal characteristics of each building at the Kangwon National University Samcheok Campus as detected using the visible and thermal images from the drone. Faulty modules detected from the temperature distribution and relative temperature differences of the PV modules were found in all four buildings. In the case of building E5, building E4, and building G, hot spots (cells with higher temperatures than the surrounding cells, indicated by white and yellow areas in the thermal image) and PID failures (single cells with higher temperatures than the surrounding cells and irregular patterns) were detected, whereas open shorts (certain strings or modules with higher temperatures than other strings or modules) were detected in building J. In the case of the study area, the visible-light images did not show any significant features, making it difficult to determine the fault, whereas the thermal images showed that the temperature of a particular cell was higher in comparison to that of the surrounding cells, thus indicating that the module was faulty.

Such defects in PV modules can cause various failures or decreases in system performance and power generation. The hot spots on the rooftop PV cells of the fifth and fourth buildings and building G were caused by cell defects, breakage, or internal connections. The PVFS reports that hotspot failures could directly cause fires, whilst defects have various effects on performance. In the case of PIDs, defects can also directly cause fires and are known to have catastrophic effects on performance. An open short in the rooftop PV cell in the lab is a case where the module system is not connected, and the fault can have a severe effect on the performance.

Table 5 shows the number of modules per building, number of faulty modules, and the ratio of healthy to faulty modules. The highest percentage of defective modules was 12% in building J, followed by 7% in building G, and 4% in buildings E5 and E4. The management team of the PV facility on the university campus reported that they did not perform any inspections or maintenance unless power generation had decreased to almost zero. Considering this situation, it is believed that the high percentage of faulty modules in building J is due to the fact that it has been operated for the longest period of time (more than 10 years). However, in the case of building E4, which began operation in September 2021, it was inferred that defects may have occurred early, not long after the start of power generation.

Defective PV modules can result in reduced power generation. For commercial PV farms, in which PV power generation is directly tied to revenue, module failure detection and active maintenance are typically performed. On the other hand, university campuses strive to create a green campus to comply with government policies and improve their internal and external image; however, considering that they do not aim to maximize power generation revenue, they often simply monitor for module failures.

4.2. Comparative Analysis of Power Generation Reduction as a Function of the PV Module Failure Rate

Table 6 lists the corrected monthly power generation for each building when the four attribute values were equally adjusted. Building E5, with an installed capacity of 100 kW_P, generated 11,450 kWh in January. However, if the installed capacity was adjusted to 50 kW, the corrected January generation was 5725 kWh (50%). The PV modules in building E5 had an initial power generation efficiency of 98.5% (empirical data for module performance in the first year of installation provided by the manufacturer), which decreased by 0.5% per year; after four years, they had a power generation efficiency of 96.5%. Considering that the modules in the other buildings were of different models and had different power generation efficiencies, we recalculated the monthly power generation in 2022, assuming a module efficiency of 100% as of 2022; that is, 100% divided by 96.5% (=100%/96.5%), which was approximately 1.036, multiplied by the original power generation of 5725 kWh, totaling 5933 kWh. Thus, each building's monthly generation was multiplied by the capacity correction factor and the generation efficiency reduction correction factor to calculate the corrected generation.

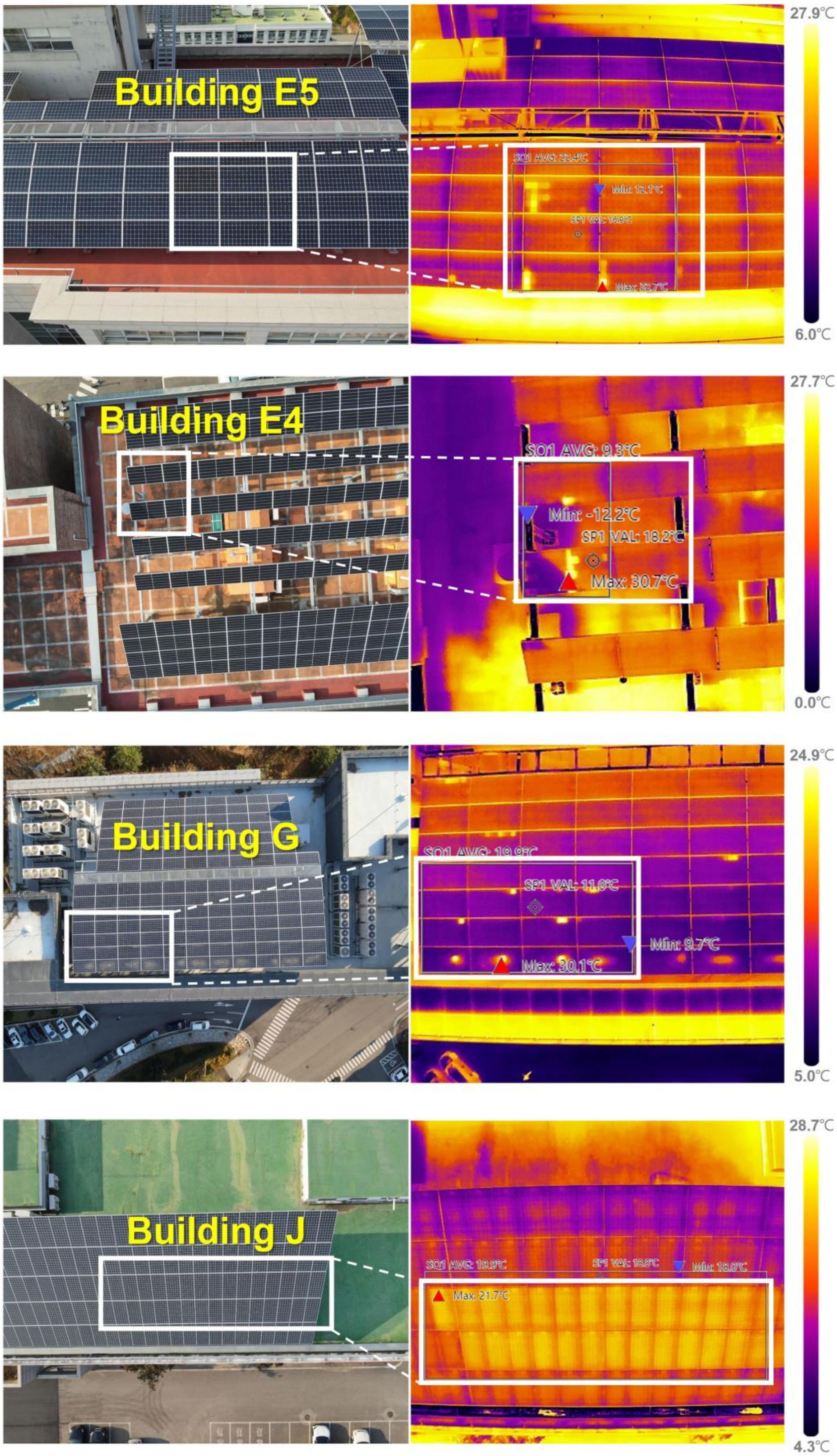

Figure 3. Photos of the defective PV modules of each building taken using drone-based infrared thermography.

Table 5. Number and proportion of defective modules of each building.

Building Name	Failure Type	No. of Module All	No. of Module Defective	Proportion (%)	Operation Period (Year)
E5	Hot spot, PID	264	12	4	4
E4		154	7	4	1
G		169	13	7	3
J	Open short fault	290	36	12	15

Table 6. Modified monthly power generation of each building considering the calibration of different capacities, degradations, tilts, and azimuths of PV systems.

Month	Original Properties (kWh)				Revised Properties (kWh)			
	E5	E4	G	J	E5	E4	G	J
January	11,450	3488	6068	2924	5933	2604	4706	3408
February	13,467	5807	6527	4518	6978	4336	5062	5266
March	13,305	8598	4281	3581	6894	6421	3320	4174
April	15,726	10,658	9726	3694	8148	7959	7543	4305
May	15,221	11,512	10,456	4451	7887	8597	8109	5188
June	13,772	8911	8374	4470	7136	6655	6494	5210
July	13,154	8097	7577	3395	6815	6047	5876	3957
August	11,155	6892	6369	3281	5780	5146	4939	3824
September	12,636	8016	6850	4088	6547	5986	5312	4765
October	10,600	6320	4789	3841	5492	4720	3714	4477
November	9460	6235	4340	2814	4901	4656	3365	3280
December	9913	6139	5006	4079	5136	4585	3883	4754
Sum	149,860	90,673	80,361	45,136	77,648	67,710	62,324	52,606

Modified properties: capacity (50 kW_P), degradation (100%), tilt (25°), azimuth (142°).

As listed in Table 4, the tilt angle of the rooftop PV modules of each building was adjusted to 25°, whilst the azimuth angle was adjusted to 142°, and the power generation was corrected accordingly. Power generation correction by adjusting the tilt angle and azimuth angle is not as simple as power generation correction by reducing the facility capacity and degradation by aging. In this study, SAM (system advisor model) software was used to predict power generation under the original conditions (tilt angle and orientation angle) and then this was compared with the power generation under the revised conditions to derive the coefficient of determination (R^2) [44] and the trend equation (Figure 4) between two power generation value sets. For example, in the case of the power generation of building G, the coefficient of determination for two power generation sets under the original properties ($X_{14–180}$) and revised properties ($X_{25–142}$) was calculated to be 0.9997, indicating that the accuracies of predictions of the actual value ($Y_{14–180}$) were reliable.

Next, using SAM software, the module tilt angle of building G was modified and set to 25° with an orientation angle of 142° to predict the power generation ($X_{25–142}$). Additionally, the corrected monthly power generation ($Y_{25–142} = 1.0086 \times X_{25–142} - 0.0257$) was calculated by applying the trend equation derived earlier. Thus, power generation due to tilt and orientation angle adjustments was corrected for all buildings. The intent is to convey that if the predicted and measured power generation of the PV modules at a given tilt and orientation angle are highly correlated, it is reasonable to extrapolate from the predicted value in areas where there are no measured values. However, in the case of building E4, the inclination angle of each string was divided between 25° and 15°. Therefore, the coefficient of determination and trend equation were obtained in the same manner as above for the string with an inclination angle of 15° and calibrated to a level of power generation at 25°.

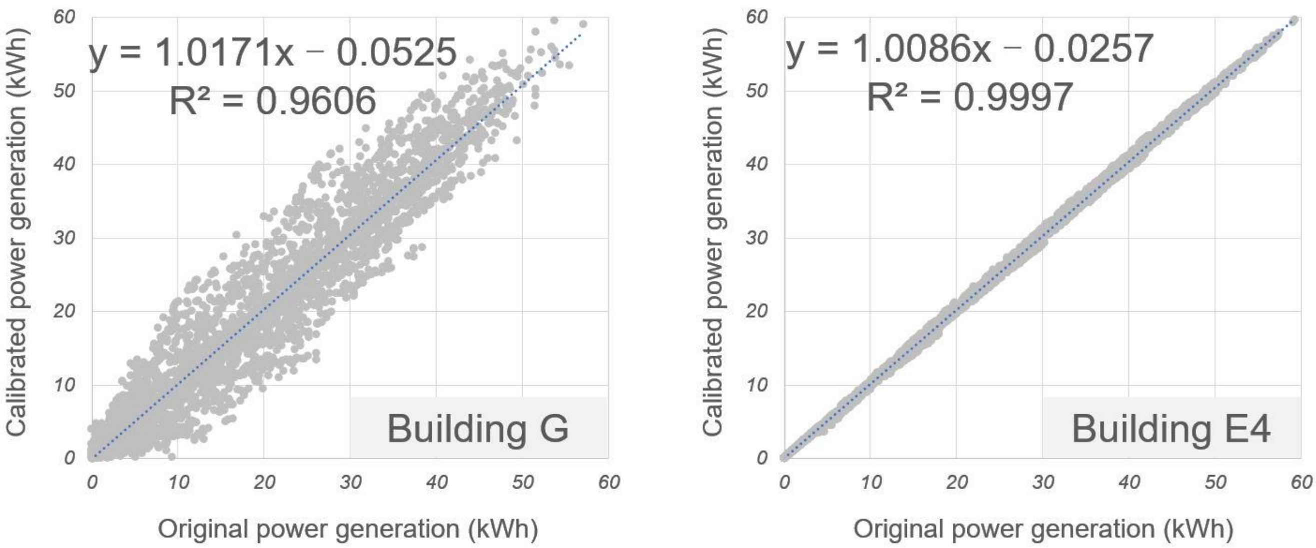

Figure 4. Correlation analysis between observed and predicted power generation using SAM software for buildings G and E4 (for evaluating the reliability of modified power generation according to the unification of the tilt and azimuth of PV modules).

The change in the PV power generation of the four buildings according to the adjusted values of the capacity, degradation, tilt, and orientation angle of the rooftop PV systems (presented in Table 4) are shown in Figure 5. It was found that in the first step, the installed capacities of buildings E5, E4, and G were changed to 50 kW_p, and the power generation decreased accordingly. On the other hand, for building J, the original capacity and the adjusted capacity were identical, so there was no change in power generation. In the second step, degradation of all buildings' PV systems was adjusted to 100%. Thus, the power generation of all buildings was changed. In the last step, power generation of buildings G and E4 was partially adjusted because only the tilt and orientation angle were adjusted.

Figure 6 shows the percentage of faulty modules for each building in the study area alongside the calibrated 2022 generation under the same conditions. Building E5, which had the lowest proportion of faulty modules, generated the most power, whereas building J, which had the highest proportion of faulty modules, generated the least. That is, the proportions of faulty modules and power generation were inversely related, and it could be clearly observed that faulty modules had an impact on power generation.

Under identical conditions for all four rooftop PV systems, the power generation of buildings E4 and E5 with the same 4% of faulty modules should be the same. However, the power generation of E5 is higher than that of E4. To interpret the reason for this, a comparison of the calibrated power generation for buildings E5 and E4 is shown by in Figure 7, which includes data from the end of 2021 to the end of 2022 when rooftop PV power values for building E4 began to be monitored. The power generation graphs followed a similar pattern for approximately 13 months, except for January and February 2022. We concluded that the calibrated generation data were reliable since patterns of power generation were similar under the same conditions (i.e., capacity, degradation, and tilt and azimuth angles). The reason for the difference in the actual generation, despite the same 4% defective panel rate, was attributed to the missing data for the first two months of 2022 for building E4.

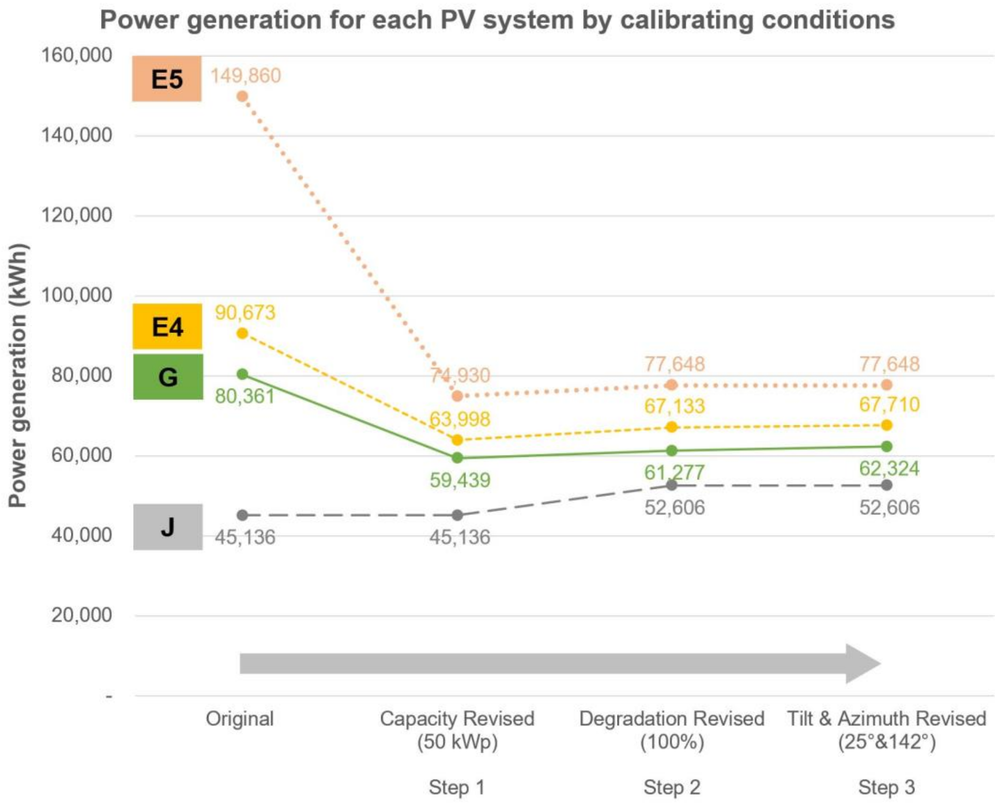

Figure 5. Change in power generation over 2022 for each PV system after unifying four conditions.

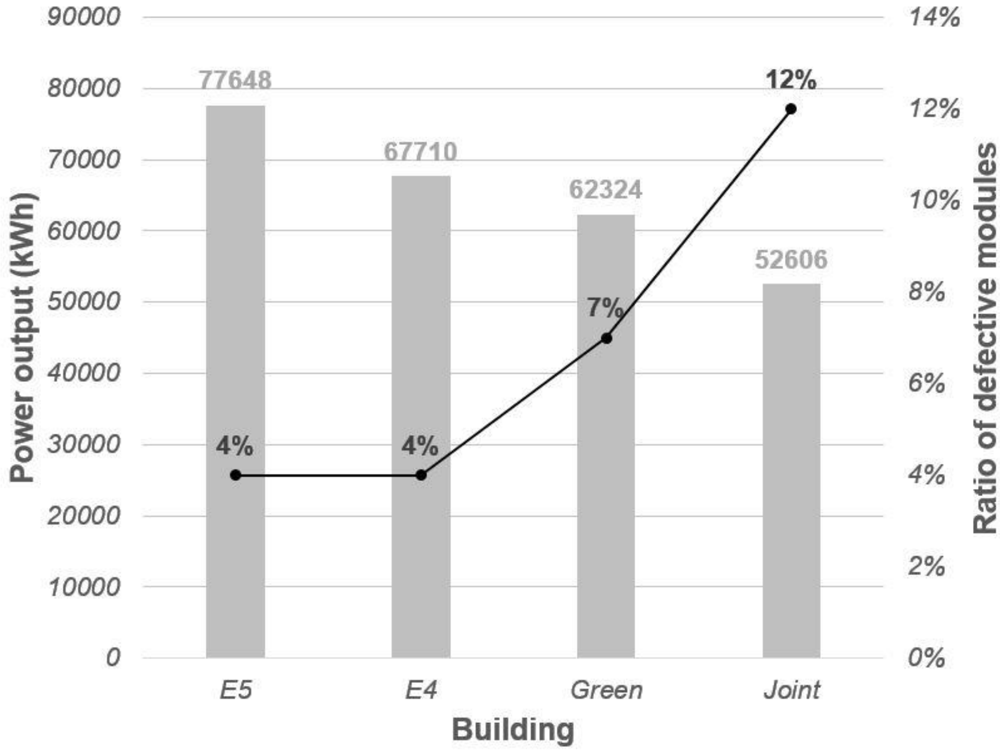

Figure 6. Comparison of defective panel ratios and power generation reductions for each building.

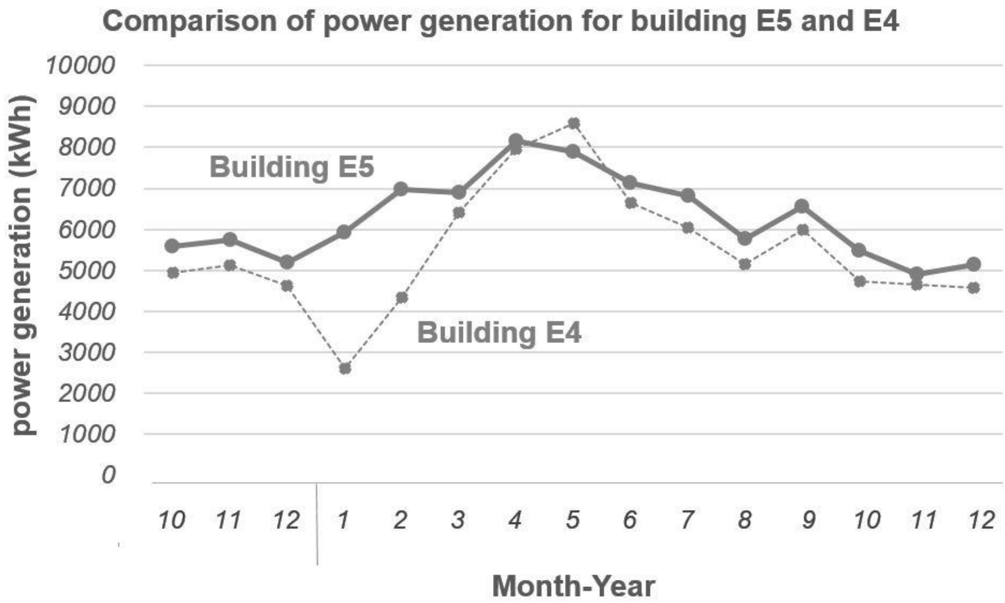

Figure 7. Comparison of the monthly power generation of building E5 and building E4.

5. Discussion

Figure 8 shows the four-year calibrated power generation for the buildings with the highest percentage of failed PV modules (building J) and the lowest percentage (building E5). From the end of 2018 to mid-2021, the analysis showed that the two buildings exhibited similar patterns of variation in power generation, with the differences in power generation being negligible. This suggested that the module failure rates of both buildings were similar. However, after the end of 2021, the two buildings exhibited some similarities in their power generation patterns, although the difference in power generation was clearly visible. For approximately one year (August 2021 to December 2022), the difference in power generation between building J and the building E5 was 33,292 kWh. This suggests that a new (or additional) module failure will occur by the end of 2021 in a shared lab.

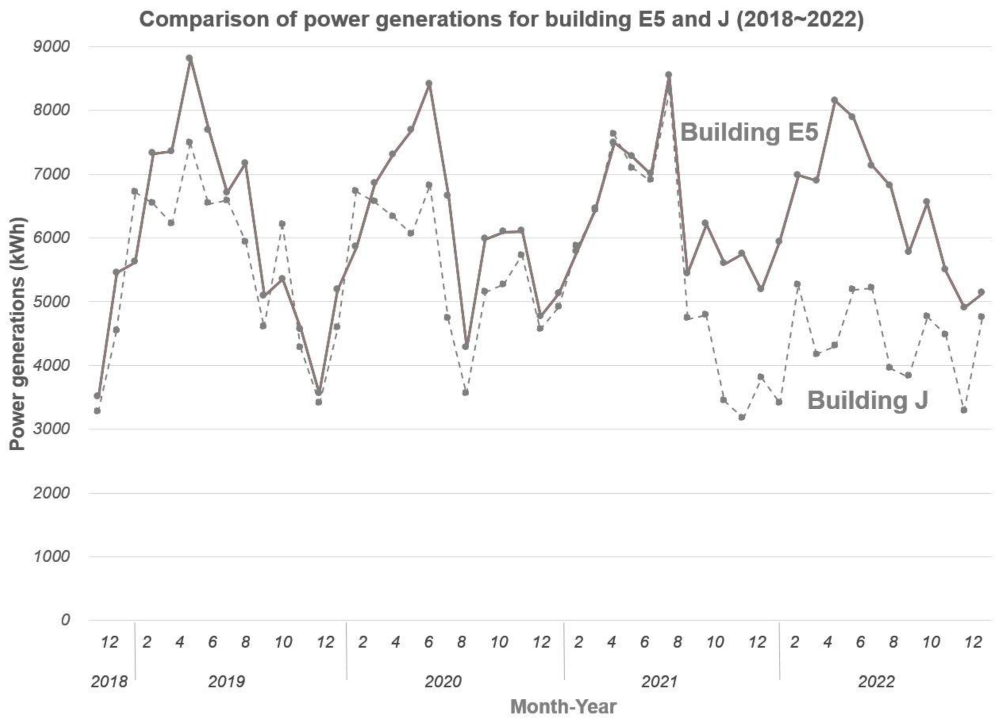

Figure 8. Comparison of monthly power output between building E5 and building J (2018–2022).

It is difficult to determine exactly when a PV panel will fail until inspecting it. Of course, if solar irradiation and high temporal resolution monitoring data are available, it is possible to detect whether the system has failures or defects by analyzing its power generation values or electrical characteristics. However, in the case of university campuses, which do not have commercial power plants, there are no high-resolution monitoring systems and periodic PV system inspections are not usually performed because of time and cost issues. Therefore, it is necessary to detect direct and indirect failures and defects of the PV module to reduce the period in which power generation is left in a degraded state.

6. Conclusions

In this study, we detected defective modules using thermal infrared images of rooftop PV modules on a university campus acquired using a thermal imaging drone. We subsequently compared and analyzed the level of power generation degradation due to the percentage of defective modules per building. Hot spots, PID, and open short-circuit faults that could not be identified through visual analysis were detected in the infrared images. The percentage of defective modules per building in the study area ranged between 4% and 12%, whilst the amount of power generation degradation increased with the percentage of suspected defective modules. In addition, a comparative analysis of the changes in power generation for buildings within the same environment allowed us to estimate when module failures may occur.

The methodology proposed in this study was insufficient for identifying the exact time of PV panel failure. To closely analyze the extent of the power generation degradation of rooftop PV facilities in each building, and its causes, accurate data on the timing of module failure are required, and further research is still needed. In this regard, solar irradiation and high-resolution power generation data are necessary for the detailed detection of PV module failures. In addition, there is a difference between theoretical panel degradation and actual panel degradation. This is because theoretical degradation values for modules are needed when predicting power generation for PV systems that have not yet been installed. Therefore, further research is needed for this also. Moreover, various studies have reported that AI technology detects defects in PV modules with higher accuracy. Therefore, it is necessary to apply AI technology to rooftop PV monitoring on university campuses in the future.

Although no new technology (i.e., machine learning or deep learning) has been developed herein, the drone-based thermal infrared imagery and power generation data analysis technique proposed in this study could detect rooftop PV module failures and provide a proper rationale for maintenance planning. It should be noted that this does not indicate that defect identification in PV modules installed on university campuses should be performed with different procedures than for commercial PV plants. Furthermore, this study can provide a useful basis for minimizing power-generation losses owing to poor maintenance. On the other hand, university campuses strive to create green campuses to respond to government policies whilst improving their internal and external image; however, since they do not aim to maximize power generation revenue, they often simply monitor panel failures. From this perspective, the results of this study can contribute to improving awareness of the need for the active maintenance of energy infrastructure to create sustainable green campuses.

Author Contributions: J.S. designed the research; K.C. gathered and processed data; All the authors interpreted the data and wrote the paper; J.S. implemented the final work for the paper submission. All authors have read and agreed to the published version of the manuscript.

Funding: This research was supported by (1) "Regional Innovation Strategy (RIS)" through the National Research Foundation of Korea (NRF) funded by the Ministry of Education (MOE) (2022RIS-005), (2) the Korea Institute of Energy Technology Evaluation and Planning (KETEP) and the Ministry of Trade, Industry & Energy (MOTIE) of the Republic of Korea (No. 20224000000080), and (3) Basic Science Research Program through the National Research Foundation of Korea (NRF) funded by the Ministry of Education (2019R1I1A3A01062541).

Data Availability Statement: Data sharing not applicable.

Conflicts of Interest: The authors declare no conflict of interest.

Abbreviations

The following abbreviations are used in this manuscript.

PV	photovoltaic
PID	potential-induced degradation
UAVs	unmanned aerial vehicles
DJI	Da Jiang Innovation
IEC	International Electrotechnical Commission
PVFS	photovoltaic failure act sheet
SAM	system advisor model

References

1. Köntges, M.; Kurtz, S.; Packard, C.E.; Jahn, U.; Berger, K.A.; Kato, K.; Friesen, T.; Liu, H.; Van Iseghem, M. *Review of Failures of Photovoltaic Modules*; Report IEA-PVPS T13-01:2014; International Energy Agency: Paris, France, 2014.
2. Khalil, I.U.; Ul-Haq, A.; Mahmoud, Y.; Jalal, M.; Aamir, M.; Ahsan, M.U.; Mehmood, K. Comparative Analysis of Photovoltaic Faults and Performance Evaluation of Its Detection Techniques. *IEEE Access* **2020**, *8*, 26676–26700. [CrossRef]
3. Köntges, M.; Oreski, G.; Jahn, U.; Herz, M.; Hacke, P.; Weiß, K.A. *Assessment of Photovoltaic Module Failures in the Field*; Report IEA-PVPS T13-09:2017; International Energy Agency: Paris, France, 2017.
4. Herz, M.; Friesen, G.; Jahn, U.; Köntges, M.; Lindig, S.; Moser, D. *Quantification of Technical Risks in PV Power Systems*; Report IEA-PVPS T13-23:2021; International Energy Agency: Paris, France, 2021.
5. Seo, H.; Suh, J. Optimal layout design according to potential assessment of rooftop photovoltaic system on southeast-facing buildings for establishing green campus. *J. Korean Soc. Miner. Energy Resour. Eng.* **2020**, *57*, 600–608. [CrossRef]
6. Nematollahi, O.; Kim, K.C. A feasibility study of solar energy in South Korea. *Renew. Sustain. Energy Rev.* **2017**, *77*, 566–579. [CrossRef]
7. Thaib, R.; Amudy, M.; Rizal, T.A. Study on Implementation of Rooftop Photovoltaic Power Plant as an Effort to Attain a Sustainable Campus. *Eur. J. Eng. Technol. Res.* **2019**, *4*, 21–25. [CrossRef]
8. Teah, H.S.; Yang, Q.; Onuki, M.; Teah, H.Y. Incorporating External Effects into Project Sustainability Assessments: The Case of a Green Campus Initiative Based on a Solar PV System. *Sustainability* **2019**, *11*, 5786. [CrossRef]
9. Baitule, A.S.; Sudhakar, K. Solar powered green campus: A simulation study. *Int. J. Low-Carbon Technol.* **2017**, *12*, 400–410. [CrossRef]
10. Yadav, B.K.; Rauniyar, P.K.; Sudhakar, K.; Bajracharya, T.R.; Priya, S.S. Sustainable green campus in NEPAL: 3E analysis. *Int. J. Low-Carbon Technol.* **2021**, *16*, 531–542. [CrossRef]
11. Zhu, X.; Lv, Y.; Bi, J.; Jiang, M.; Su, Y.; Du, T. Techno-Economic Analysis of Rooftop Photovoltaic System under Different Scenarios in China University Campuses. *Energies* **2023**, *16*, 3123. [CrossRef]
12. Pham, M.-H.; Phap, V.M.; Trung, N.N.; Son, T.T.; Kien, D.T.; Anh Tho, V.T. A Study on the Impact of Various Meteorological Data on the Design Performance of Rooftop Solar Power Projects in Vietnam: A Case Study of Electric Power University. *Energies* **2022**, *15*, 7149. [CrossRef]
13. Hua, L.-G.; Memon, Q.A.; Shaikh, M.F.; Shaikh, S.A.; Rahimoon, R.A.; Shah, S.H.H.; Qadir, A. Comparative Analysis of Power Output, Fill Factor, and Efficiency at Fixed and Variable Tilt Angles for Polycrystalline and Monocrystalline Photovoltaic Panels—The Case of Sukkur IBA University. *Energies* **2022**, *15*, 3917. [CrossRef]
14. Choi, Y.; Oh, M.; Kang, J.; Lutzenhiser, L. Plans and Living Practices for the Green Campus of Portland State University. *Sustainability* **2017**, *9*, 252. [CrossRef]
15. Gálvez, D.M.; Kerdan, I.G.; Carmona-Paredes, G. Assessing the Potential of Implementing a Solar-Based Distributed Energy System for a University Using the Campus Bus Stops. *Energies* **2022**, *15*, 3660. [CrossRef]
16. Cordeiro, I.; Bassi, W.; Sauer, I.L. Hosting Capacity Estimate Based on Photovoltaic Distributed Generation Deployment: A Case Study in a Campus of the University of São Paulo. *Energies* **2023**, *16*, 3934. [CrossRef]

17. Di Somma, M.; Buonanno, A.; Caliano, M.; Graditi, G.; Piazza, G.; Bracco, S.; Delfino, F. Stochastic Operation Optimization of the Smart Savona Campus as an Integrated Local Energy Community Considering Energy Costs and Carbon Emissions. *Energies* **2022**, *15*, 8418. [CrossRef]
18. Gbadamosi, S.L.; Ogunje, F.S.; Wara, S.T.; Nwulu, N.I. Techno-Economic Evaluation of a Hybrid Energy System for an Educational Institution: A Case Study. *Energies* **2022**, *15*, 5606. [CrossRef]
19. Roggi, G.; Niccolai, A.; Grimaccia, F.; Lovera, M. A Computer Vision Line-Tracking Algorithm for Automatic UAV Photovoltaic Plants Monitoring Applications. *Energies* **2020**, *13*, 838. [CrossRef]
20. Kim, D.; Youn, J.; Kim, C. Automatic Photovoltaic Panel Area Extraction from UAV Thermal Infrared Images. *J. Korean Soc. Surv. Geod. Photogramm. Cartogr.* **2016**, *34*, 559–568. [CrossRef]
21. Díaz, J.J.V.; Vlaminck, M.; Lefkaditis, D.; Vargas, S.A.O.; Luong, H. Solar panel detection within complex backgrounds using thermal images acquired by Uavs. *Sensors* **2020**, *20*, 6219. [CrossRef]
22. Jung, S.; Jo, Y.; Kim, Y.J. Aerial surveillance with low-altitude long-endurance tethered multirotor UAVs using photovoltaic power management system. *Energies* **2019**, *12*, 1323. [CrossRef]
23. Grimaccia, F.; Aghaei, M.; Mussetta, M.; Leva, S.; Quater, P.B. Planning for PV plant performance monitoring by means of unmanned aerial systems (UAS). *Int. J. Energy Environ. Eng.* **2015**, *6*, 47–54. [CrossRef]
24. Moudrý, V.; Beková, A.; Lagner, O. Evaluation of a high resolution UAV imagery model for rooftop solar irradiation estimates. *Remote Sens. Lett.* **2019**, *10*, 1077–1085. [CrossRef]
25. Kim, K.; Choi, Y.; Shim, K.; Jeon, H.; Commerford, J.; Matson, E.T. Analyzing the range of angles of a solar panel to detect defective cells, using a UAV. In Proceedings of the Third IEEE International Conference on Robotic Computing (IRC), Naples, Italy, 25–27 February 2019; pp. 471–476. [CrossRef]
26. Lee, G.S.; Lee, J.J. The Detection of Heat Emission to Solar Cell Using UAV-Based Thermal Infrared Sensor. *J. Korean Soc. Geospatial Inf. Syst.* **2017**, *25*, 71–78. [CrossRef]
27. Henry, C.; Poudel, S.; Lee, S.W.; Jeong, H. Automatic detection system of deteriorated pv modules using drone with thermal camera. *Appl. Sci.* **2020**, *10*, 3802. [CrossRef]
28. Lee, D.H.; Park, J.H. Developing inspection methodology of solar energy plants by thermal infrared sensor on board unmanned aerial vehicles. *Energies* **2019**, *12*, 2928–2941. [CrossRef]
29. Grimaccia, F.; Leva, S.; Niccolai, A. PV plant digital mapping for modules' defects detection by unmanned aerial vehicles. IET Renew. *Power Gener.* **2017**, *11*, 1221–1228. [CrossRef]
30. Cubukcu, M.; Akanalci, A. Real-time inspection and determination methods of faults on photovoltaic power systems by thermal imaging in Turkey. *Renew. Energy* **2020**, *147*, 1231–1238. [CrossRef]
31. Lee, G.-S. Test of fault detection to solar-light module using UAV based thermal infrared camera. *J. Korean Assoc. Geogr. Inf. Stud.* **2016**, *19*, 106–117. [CrossRef]
32. Quater, P.B.; Grimaccia, F.; Leva, S.; Mussetta, M.; Aghaei, M. Light unmanned aerial vehicles (UAVs) for cooperative inspection of PV plants. *IEEE J. Photovolt.* **2014**, *4*, 1107–1113. [CrossRef]
33. Zefri, Y.; Elkettani, A.; Sebari, I.; Lamallam, S.A. Thermal Infrared and Visual Inspection of Photovoltaic Installations by Uav Photogrammetry—Application Case: Morocco. *Drones* **2018**, *2*, 41. [CrossRef]
34. Liao, K.C.; Lu, J.H. Using UAV to detect solar module fault conditions of a solar power farm with IR and visual image analysis. *Appl. Sci.* **2021**, *11*, 1835. [CrossRef]
35. Li, X.; Yang, Q.; Chen, Z.; Luo, X.; Yan, W. Visible defects detection based on UAV-based inspection in large-scale photovoltaic systems. *IET Renew. Power Gener.* **2017**, *11*, 1234–1244. [CrossRef]
36. Akram, M.W.; Li, G.; Jin, Y.; Chen, X.; Zhu, C.; Ahmad, A. Automatic detection of photovoltaic module defects in infrared images with isolated and develop-model transfer deep learning. *Sol. Energy* **2020**, *198*, 175–186. [CrossRef]
37. Wang, X.; Yang, W.; Qin, B.; Wei, K.; Ma, Y.; Zhang, D. Intelligent monitoring of photovoltaic panels based on infrared detection. *Energy Rep.* **2022**, *8*, 5005–5015. [CrossRef]
38. Tsanakas, J.A.; Ha, L.; Buerhop, C. Faults and infrared thermographic diagnosis in operating c-Si photovoltaic modules: A review of research and future challenges. *Renew. Sustain. Energy Rev.* **2016**, *62*, 695–709. [CrossRef]
39. Ali, M.U.; Khan, H.F.; Masud, M.; Kallu, K.D.; Zafar, A. A machine learning framework to identify the hotspot in photovoltaic module using infrared thermography. *Sol. Energy* **2020**, *208*, 643–651. [CrossRef]
40. Niazi, K.A.K.; Akhtar, W.; Khan, H.A.; Yang, Y.; Athar, S. Hotspot diagnosis for solar photovoltaic modules using a Naive Bayes classifier. *Sol. Energy* **2019**, *190*, 34–43. [CrossRef]
41. Starzyński, J.; Zawadzki, P.; Harańczyk, D. Machine Learning in Solar Plants Inspection Automation. *Energies* **2022**, *15*, 5966. [CrossRef]
42. IEC (International Electrotechnical Commission). Available online: https://webstore.iec.ch/publication/28628/ (accessed on 27 February 2023).

43. DJI Mavic 2 Enterprise Advanced. Available online: https://www.dji.com/mavic-2-enterprise-advanced/ (accessed on 27 February 2023).
44. Di Bucchianico, A. Coefficient of Determination (R^2). In *Encyclopedia of Statistics in Quality and Reliability*; Wiley: Hoboken, NJ, USA, 2007.